Boletín Geológico

SERVICIO GEOLÓGICO COLOMBIANO

Boletín Geológico, 48(1), 123-97, 2021,
https://doi.org/10.32685/0120-1425/bol.geol.48.1.2021.504

Received: May 15, 2020

Revised: August 14, 2020

Accepted: March 2, 2021

Published online: July 12, 2021

Graphical representation of structural data in the field: A methodological proposal for application in deformed areas

Representación gráfica de datos estructurales en campo: Una propuesta metodológica para su aplicación en áreas deformadas

Julián Andrés **López Isaza**[1], Mario Andrés **Cuéllar Cárdenas**[1], Lina María **Cetina Tarazona**[1], Anny Julieth **Forero Ortega**[1], Ana Milena **Suárez Arias**[1], Óscar Freddy **Muñoz Rodríguez**[1], Luis Miguel **Aguirre Hoyos**[1], María Juliana **Gutiérrez López**

1 Dirección de Geociencias Básicas, Servicio Geológico Colombiano, Bogotá, Colombia.
Corresponding author: Julián Andrés López, jlopez@sgc.gov.co

Abstract

The description of the fabric elements represented by the linear and planar structures present at different scales is a key component of fieldwork. A scheme is proposed for the systematic registration of planes and lineations, coded as S (planar surfaces), F (folds), and L (lineations), among others, that allows for the orderly storage of the measurements taken. This scheme includes information related to the kinematics, the kinematic indicators, and the certainty or reliability ascribed to the assigned movement. In the fieldwork, the graphic representation of the structural measures in modified projection nets includes concentric circles for each dip. Direct drawing of the outcrop data is undertaken, dispensing with the use of tracing or transparent paper. The stereograms resulting from the graphic representation in the modified Wulff stereographic projection net, and the modified Schmidt equal-area net, can be complemented by rose diagrams for visualization of the spatial ordering. During field campaigns in the outcrops, it is essential to visualize the spatial orientation of the data in the diagrams to determine the main structural trends, the vergence, the kinematic nature of faults and shear zones, paleo-stress tensors, and to differentiate structural domains, among others. This information supports the reconstruction of geological and tectonic history and the establishment of relationships between the different geological processes.

Keywords: Structural analysis, structural data, stereographic projection, equal-area projection, rose diagram, fabric elements.

Citation: López Isaza, J. A., Cuéllar Cárdenas, M. A., Cetina Tarazona, L. M., Forero Ortega, A. J., Suárez Arias, A. M. Muñoz Rodríguez, O. F., Muñoz Rodríguez, O. F., Aguirre Hoyos, L. M., & Gutiérrez López, M. J. (2021). Graphical representation of structural data in the field: A methodological proposal for its application in deformed areas. *Boletín Geológico, 48*(1), 123-139. https://doi.org/10.32685/0120-1425/bol.geol.48.1.2021.504

Resumen

La descripción de los elementos de fábrica representados por las estructuras lineales y planares presentes a diferentes escalas es uno de los aspectos más relevantes del trabajo de campo. Así, para el registro sistemático de planos y lineaciones, codificados como S (superficies planas), F (pliegues), L (lineamientos), entre otros, se propone un esquema que permite el almacenamiento ordenado de las mediciones realizadas. Este esquema incluye información relacionada con la cinemática, los indicadores cinemáticos y la certeza o confiabilidad que se otorga al movimiento asignado. Durante el trabajo de campo, la representación gráfica de las mediciones estructurales se realiza en redes de proyección modificadas que incluyen círculos concéntricos para cada buzamiento, y permiten dibujar al trazo los datos estructurales en el afloramiento, prescindiendo del uso de papel de calco o transparente. Como tal, los estereogramas resultantes de la representación gráfica en la red de proyección estereográfica de Wulff modificada, y la red de igual área de Schmidt modificada, deben complementarse con diagramas rosa para la visualización del ordenamiento espacial. Durante las campañas de campo, en los afloramientos es fundamental visualizar la orientación espacial de los datos en los diagramas para determinar las principales tendencias estructurales, la vergencia, el sentido cinemático de fallas y zonas de cizallamiento, los tensores de paleo-esfuerzo, y diferenciar dominios estructurales, entre otros factores. Esta información apoya la reconstrucción de la historia geológica y tectónica y el establecimiento de las relaciones entre los diferentes procesos geológicos.

Palabras clave: Registro de datos estructurales, red de proyección modificada, proyección estereográfica, proyección de igual área, diagrama rosa, elementos de fábrica.

1. Introduction

Analysis of the spatial location of geological structures acquired in the field using graphical techniques during mapping campaigns is of vital importance for determining the direction of tectonic drag, the kinematics of shear zones and paleostress tensors, and axes of elongation and shortening; and to define the deformation phases recorded by lithological units. This makes it possible to reconstruct geological and tectonic history as well as establish relationships between different geological processes (Turner and Weiss, 1963; McClay, 1987; Passchier et al., 1990; Hatcher, 1995; Hopgood, 1999; Passchier and Trouw, 2005; Babín and Gómez, 2010a; Fossen, 2010; López and Zuluaga, 2012; Compton, 2016; Fossen et al., 2019; Fossen, 2019). Traditionally, to determine the spatial orientation of fabric elements, the horizontal and vertical angular relationships of geological structures are measured using analog geological compasses, and the data thus acquired are recorded in field notebooks.

The acquisition and storage of structural data is possible with the use of different mobile devices subject to connection availability, through the implementation of applications (apps) such as *Stereonet Mobile, eGEO Compass Pro*, *GeoClino for iPhone*, *Geological Compass Full*, *Lambert*, and *Structural Compass*. This makes it possible to obtain a quick record of the orientation of geological structures and to evaluate the uncertainty, from the visualization of the spatial distribution of the data in stereograms. It is also possible to obtain the location of the points or stations where the structural data are taken on digital map platforms, by means of positioning systems included in mobile devices, and their visualization is possible in viewers, such as *Google Earth*, or apps compatible with geographic information systems, such as *Mobile Data Collection*, *CartoDruid*, *MAPit*, *Nextgis* and *Qfield for Qgis*, and *ArcGIS Explorer* and *Collector for ArcGIS*. Describing each of the aforementioned applications is beyond the scope of this article, but the interested reader is referred to Allmendinger et al. (2017), Novakova and Pavlis (2017), Lee et al. (2018), and Whitmeyer et al. (2019), among others, as well as the respective descriptions provided by the developers.

For the discrimination, recording, and description of data pertaining to different structures, basic concepts are used and applied from different structural geology texts (Hills, 1972; Hobbs et al., 1976; Blés, 1977; Bartlett et al., 1981; Hancock, 1985; McClay, 1987; Marshak and Mitra, 1988; Price and Cosgrove, 1990; Hatcher, 1995; Ragan, 2009; Babín and Gómez, 2010b and c; Allmendinger, 2019). However, it is important to keep in mind the methodical and orderly recording of the data acquired in the field, since, particularly when they are not measured with mobile devices (which by default integrate the data in tables), they should allow differentiating the types of data and structures measured (e.g., foliation, cleavage, fault

plane, mineral lineation, striation, and fold axes), as well as including parameters for rating certainty or reliability (quantitative or qualitative) vis-à-vis kinematics of faults and shear zones. Whether and the extent to which data logging is undertaken appropriately depends on the nature and extent of the geologist´s experience as well as the complexity of the task. If it is assumed that the data will be analyzed using some specialized software (such as Tectonics FP written and developed by Reiter, F. and Acs, P. http://www.tectonicsfp.com, Ortner et al. (2002); TectonicVB written and developed by Ortner, H. https://www.uibk.ac.at/geologie/tvb/front.html, Ortner et al. (2002); Stereonet written and developed by Allmendinger, R. https://www.rickallmendinger.net, Allmendinger et al. (2012) and Cardozo and Allmendinger (2013); GEOrient written and developed by Holcombe, R. https://www.holcombe.net.au/software/georient.html, Holcombe (2015); Faultkin written and developed by Allmendinger, R. https://www.rickallmendinger.net, Marrett and Allmendinger (1990) and Allmendinger et al. (2012); Win-Tensor written and developed by Delvaux, D. http://damiendelvaux.be/Tensor/WinTensor/win-tensor.html, Delvaux and Sperner (2003); and T-Tecto written and developed by Žalohar, J. https://quantectum.com/t-tecto/, Žalohar and Vrabec (2007)), then parameters for assigning certainty to kinematics must be taken into account.

There are different notations and conventions for the recording of structural data taken in the field (McClay, 1987), among which the azimuthal conventions or azimuth of dip, right hand rule, quadrants, and the convention given by dip (inclination of the plane)®azimuth of dip (direction of inclination) or dip direction stand out. Additionally, to gauge the representativeness of the structural data acquired in the field, the following should be described: the types of structures investigated, the shear relationships between them, the lithology analyzed, and the uncertainties generated by the surface irregularities of the structure planes. Some questions that are very common among students, researchers, and other professionals faced with carrying out work with emphasis on structural geology, especially at sites where it is not possible to use mobile devices, are as follows. What structural variables should be measured? How should data be recorded during a field campaign? How much data should be acquired on average? To answer some of these questions, in this paper we present a proposal for the rapid recording and graphical visualization of structural data acquired in the field directly in the outcrop. To this end, we propose a scheme (either by means of analog compasses or with mobile devices to complement the information) that allows their arrangement by type of fabric element (planar or linear), including a qualitative rating of the certainty or reliability of the kinematics assigned to the direction of movement of shear zones (Delvaux and Sperner, 2003; Žalohar, 2020).

In addition, during the field campaign, spatial visualization of strike-dip relationships of geological structures directly in outcrops is realized by plotting structural data from the application of conventional methods facilitated by stereographic projection grids, as a graphical alternative to represent three-dimensional data in a two-dimensional way (Bucher, 1944; Ramsay, 1967; Sander, 1970; Chica, 1984). This implies the dedication of time in the field to obtain a sufficiently representative amount of data for the stereograms. A stereographic projection network allows representing orientations of planes and lines with respect to the center of a sphere on an equatorial projection plane, combining spherical and azimuthal projections (Phillips, 1973; Lisle and Leyshon, 2004; Babín and Gómez, 2010a).

For conventional graphical representation of structural data in the field, especially in areas where it is not possible to use mobile devices for data visualization purposes, it is necessary to have a stereographic grid at hand (available in many structural geology textbooks) and paper (transparent or tracing) which is rotated over the fixed grid to plot the data (Phillips, 1973; Allmendinger, 2019). This process can be streamlined by using a modified stereographic template that allows the data to be plotted directly, i.e., dispensing with paper that must be rotated over the stereographic template. Taking into account the need to ensure that the graphical representation of structural data directly in the outcrop is done effectively and efficiently, in this article we propose the use of a modified stereographic projection grid that facilitates the direct plotting of the data, dispensing with the use of transparent / tracing paper. This is complemented with the elaboration of rose diagrams or histograms of circular frequencies that allow visualizing the main trends of the structures in the field. This makes it possible to establish the direction of tectonic drag (among other important considerations for accurate interpretation in the field), to formulate hypotheses, and to have a general understanding of the paleo-stress field.

2. Recording of data acquired in the field

Structural characterization in deformed areas includes the study of fabric elements represented by linear structures (e.g., mineral lineations, axial axes of folds or microfolds, and slickenside linea-

tions or slickenlines) and planar structures (e.g., stratification, joints, cleavages, and fault planes), which are described during fieldwork, in addition to the establishment of the relationships between them, the mechanics of the deformation, their temporalities, and the structural level of the crust in which they developed (Turner and Weiss, 1963; Roberts, 1982; Wilson, 1982; Passchier *et al*., 1990; Price and Cosgrove, 1990; Hatcher, 1995; Hopgood, 1999; Van der Pluijm and Marshak, 2004; Fossen, 2010). A fact of particular importance for descriptions of geologic structures is that one should have control, as far as possible, of the three-dimensional layout of the structure. The most accepted convention for the recording of structures generated from progressive deformation, deformation phases, and superposition of deformation events classifies structures by type, discriminating the fabric elements (planes and lineations) including the relative temporal order of the formation of the structures (Turner and Weiss, 1963; Marshak and Mitra, 1988; Passchier and Trouw, 2005).

In this sense, the fabric elements are distinguished as 'S' for planar surfaces, 'F' for folding, 'L' for lineations, 'J' for joints, 'V' for veins and veinlets, 'D' for deformations, and 'M' for metamorphic events (Sander, 1911; Turner and Weiss, 1963; McClay, 1987; Marshak and Mitra, 1988; Passchier and Trouw, 2005). The temporal order between the developed structures is defined according to their shear relationships, and in this sense, they are recorded from oldest to most recent, as $_{-0}$ (when the structure is primary) to -n (Turner and Weiss, 1963; Passchier and Trouw, 2005). Planar structures are denoted S_0 when they correspond to layering, and S_1 to S_n when they are overlapping planes and include foliations, whereas folds, lineations, joints, veins and veinlets, deformations, and metamorphic events range from $_{-1}$ to $_{-n}$ (cf. McClay, 1987; Marshak and Mitra, 1988; Price and Cosgrove, 1990; Passchier and Trouw, 2005).

Since exact determination of structure types is fundamental for the visualization of the structural data in the field, a scheme for recording the different fabric elements, planar or linear, is proposed, so that the information can be properly ordered (Table 1). This scheme considers the ordered recording of the planar and linear fabric elements, differentiating the main data groups, which include the different types of planar structures and lineations. The proposed model includes two columns for recording planar structures and lineations, one for the structural data, regardless of the notation used, and another for the type of structure, either planar or lineation. It is suggested that, where required, the recording of lineations should always be undertaken in front of the datum of the plane containing them, which is essential when recording striations that demarcate the direction of displacement (e.g., slickenside lineations or slickenlines) associated with fault planes, or when recording lineations associated with foliations (e.g., mineral lineation). On the other hand, it is also important, as far as possible, to specify the frequency, intensity, and spacing between fault planes. Additionally, for faults, it is necessary to include the data corresponding to the kinematics or direction of movement, including the indicators that support the kinematics, and an assessment of the certainty or reliability of the kinematics assigned to the direction of movement.

Among the fabric elements, planes (or planar surfaces) include layering (S_0), cleavage (S1 - S_n), compaction cleavage, dissolution pressure (stylolites and slickolites), disjunctive, pencil, slate, hinge or axial plane, phyllitic, crenulation, as well as other types of foliations (S_{n+1} - S_{n+n}), such as schistosity, gneissic foliation, banding, transposition and/or mylonitic foliation, shear band cleavage (C), deformation bands, joints (J), magmatic or flow foliation, shears and fault planes, friction or slickensides, contacts, and veins and dykes. Lineations (L) can be discrete structural or stretching (oriented pebbles, ooids, fossils, and alteration spots), constrained structural (intersections, charnels, boudins, mullions, and slip), or polycrystalline mineral lineations (rods, mineral aggregates, mineral slickenlines, and non-fibrous overgrowth), and grain or monomineral (acicular habit, elongation, and mineral fibers), among others.

For the recording of structural data of faults and shear zones, different considerations must be taken into account, including the type of shear (fault planes), the determination of the kinematics or direction of movement, with their respective indicators, and the assignment of the level of certainty or reliability of the kinematics. The latter is of particular importance for subsequent data processing in specialized software. The shear types (and failure planes) included in brittle shear zones can be described as *principal shears* (Y), which accommodate most of the displacement and are parallel to the main direction of motion in a shear zone, synthetic Riedel shears (R) oriented with angles equivalent to half the angle of internal friction, antithetic Riedel shears (R') oriented with angles equal to the difference of the subtraction of 90° and half the angle of internal friction, tension fractures (T) oriented with angles of 45° with respect to the main direction of motion, and synthetic (P) and antithetic (P' or X) post-Riedel shears (Figure 1). On the other hand, the development of step veins (*en echelon*), kink bands, and antifractures is also common in shear zones; and in ductile shear zones the limits of the shear zone and the foliations contained in them are recorded.

Table 1. Proposed data recording scheme for measurements undertaken on planar and linear fabric elements during field campaigns.

Plane		Lineation		Movement direction and Sense of shear	
Structural data	**Planar type[1]**	**Structural data**	**Lineation type**	**Kinematic**	**Assurance level**
	Planar fabric elements				
	S_0		Linear fabric elements		
	$S_1 - S_n$		Mineral lineation		
	$S_{n+1} - S_{n+n}$		Hinge line of folds		
	Axial surface or hinge plane		Crenulation		
Dip Direction (*Dip→Dir*)[2]	Veins		Intersection lineation		
	Contacts	Plunge → Az. Plunge[2]			
Quadrants	Joints (J)				
Right hand rule		Pitch or Rake and pitching sense		Right lateral or dextral	
				Left lateral or sinistral	Low (Kinematic: supposed)
Strike Azimuth	Slickenside plane or fault plane		Slickenline	Normal	Medium (Kinematic: Possible or Probable)
	Riedel shear type (Y, R, R', P, T, X)		Slickenside-related features	Reverse Thrust	High (Kinematic: True)
			Striations	Oblique	
				Kinematic indicators[3]	

1 Includes the designation of the type of plane, i.e., Sn - foliation

2 Notation taken from McClay (1987)

3 The kinematic indicators by which the kinematics or direction of motion is determined should be recorded.

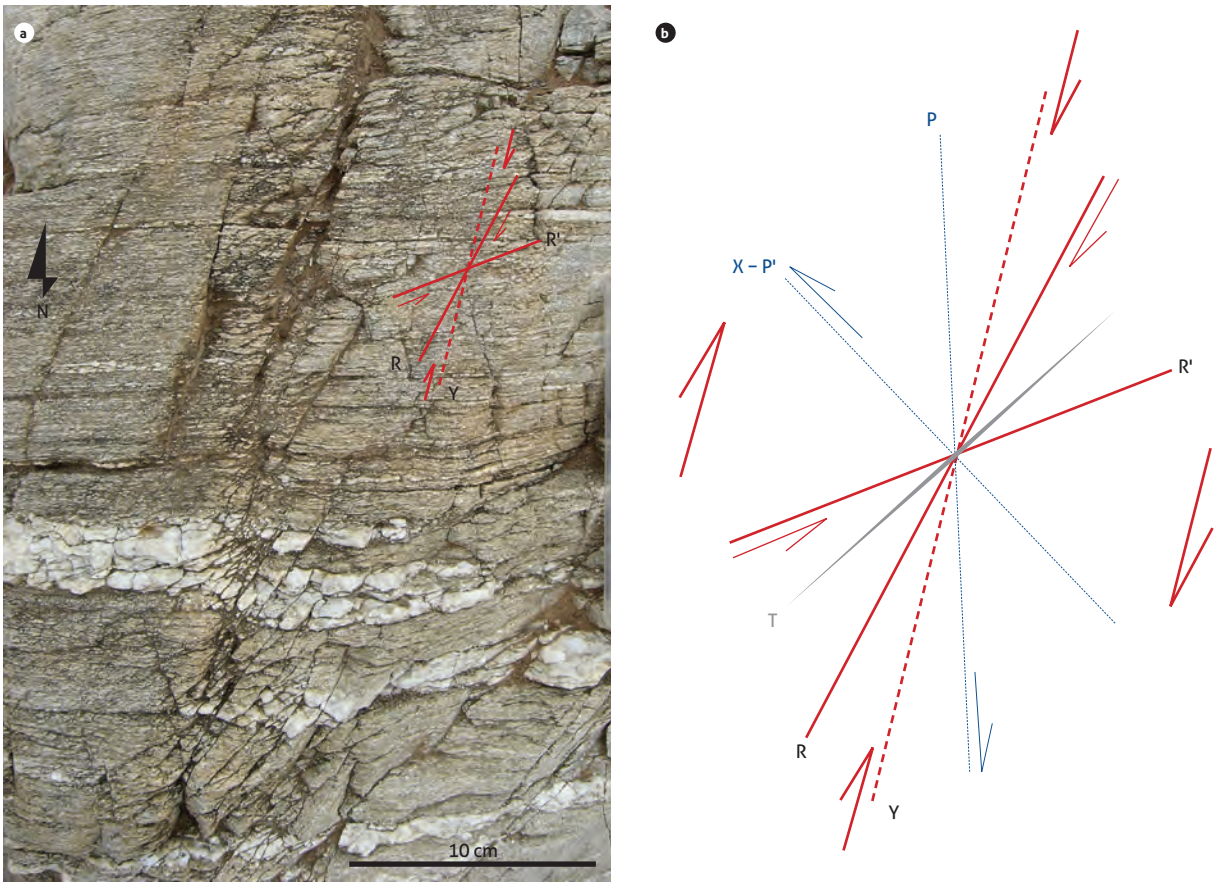

Figure 1. Interpretation of Riedel shears in outcrop
a) Distribution of synthetic and staggered antithetic Riedel shears in amphibolite outcrops belonging to the Neis de Macuira, Serranía de Simarúa, Alta Guajira. b) Schematic representation of the distribution of conjugate Riedel shears, which may be associated. R, synthetic Riedel shears. R', antithetic Riedel shears. Y, principal shears. T, tension fractures. P, post-Riedel synthetic shears. P' or X, antithetic post-Riedel shears.

In faults and shear zones, the direction of movement or kinematics can be defined as normal, reverse, strike or transcurrent, and oblique, and can be determined from kinematic or shear direction indicators on the friction or fault plane, or in sections perpendicular to the friction plane (Simpson and Schmid, 1983; Doblas, 1987; 1998; Hanmer and Passchier, 1991; Mawer, 1992; Passchier and Trouw, 2005). Accordingly, kinematic indicators are structures that allow determining the direction of movement or flow of one rock mass relative to another, both in brittle and ductile shear zones (Petit et al., 1983; Sugden, 1987; Petit, 1987; Doblas, 1987; 1998; Doblas et al., 1997 a and b; Passchier and Coelho, 2006). The most common kinematic indicators in faults and brittle shear zones that have developed on the fault plane are fault grooves, tectonic channels, slickenlines, congruent and incongruent steps, growth fibers, 'V' or crescentic markings, trails, rolling grooves, spurs, notches and normal and reverse microfractures, among others (Figure 2). On the other hand, in sections perpendicular to the friction plane, Riedel shears (T, R, and P criteria), congruent and incongruent starting steps, crystallization steps, accretion steps, tension cracks, normal and inverse microfractures, fault-produced schistosities and spurs, among others, can be differentiated. The most common kinematic indicators in ductile shear zones include shear bands and S-C-C' structures, boudinage, objects (porphyroclasts and porphyroblasts) of mantle, sigmoids, pressure shadows, flanking structures, tension veins, and folds, among others (Figure 2). However, describing the full array of kinematic indicators is beyond the scope of this paper, so the reader is referred to review the foregoing references.

Qualitative assessment of the certainty or reliability of the kinematics assigned to the direction of movement of faults and shear zones depends on kinematic indicators, which in some cases can be ambiguous, or, in other words, not all indicators are reliable, which is why it is necessary to correctly describe the observed indicators (on types of indicators and their interpretation, see Doblas, 1998). Therefore, robust indicators, such as steps with crystal fiber development, tension cracks, hybrid fractures, Riedel (synthetic and conjugated antithetic), or slickensides, associated with slickenlines, allow for obtaining a reliable sense of movement. On the other hand, kinematic indicators, such as V-shaped notches, congruent and incongruent starting steps, accretionary steps, isolated synthetic or antithetic microfractures, transposed previous foliations, and the inclination of microfractures, can lead to ambiguous or erroneous interpretations, and result in an unreliable sense of motion. Similarly, a combination of reliable and unreliable indicators results in interpretations in which a moderately reliable sense of motion is obtained, and, therefore, a medium level of certainty. Accordingly, we propose that the kinematics in the data recording table should be qualitatively ascribed as true, when the level of certainty is high; probable or possible, when the level of certainty is moderate or the indicators taken into account for the definition of the kinematics are ambiguous; and assumed, when the level of certainty is low. However, we consider that the way in which the level of certainty is designated and recorded depends to a large extent on the user's preference for particular software, since numerical or alphabetical codes may be required. On the other hand, although it is not always possible, certainty or reliability should ideally be determined from the identification of an association of different kinematic indicators that confirm the assigned direction of movement, so it is necessary to identify both those that are on the friction or failure plane, as well as those that occur in sections perpendicular to the friction plane.

3. Graphical representation of planar and linear data: Modified stereographic projection grid

To dispense with the use of transparent / tracing paper during the graphical representation of structural data in the field, the stereographic projection grid (Figure 3) has been modified to facilitate the direct plotting of structural data. More specifically, for the graphical representation of planar and linear data in the field, the Wulff (Figure 3a) and Schmidt (Figure 3b) grids were modified, including concentric circles for each inclination value (of 10°) inside the stereographic projection grid, which allows for direct plotting without rotations; in this way, visualization of the data in the outcrop is possible. This methodology simplifies the process that has traditionally been followed, in which the plotting of structural data is performed on a stereographic projection grid involving the use of tracing or transparent paper, and the plotting of the data is undertaken by rotating the paper on the stereographic projection grid (Figure 4) (Lisle and Leyshon, 2004; Ghosh, 2013).

Geometrically, stereographic grids represent the equatorial plane of a sphere viewed from the zenith. These grids are constituted by major circles, which correspond to north-south planes with different angles of inclination, passing exactly through the center of the sphere containing the equatorial plane, and by

Figure 2. Kinematic indicators of brittle and ductile shear zones
a) Fault or friction plane developed in the Santa Barbára Monzogranite, Los Curos-Guaca road, La Judia creek sector. b) Detail of fault plane with development of fault grooves (*s*). The white line is arranged parallel to the direction of the fault grooves, oblique dextral kinematics. c) Slickenlines and step-steps, Perchiquez river fault, oblique dextral kinematics. d) Beheaded folds (*p*) with boudinized flanks and development of *pinch and swell* structures (*b*) parallel to the transposition foliation, as evidence of ductile shearing, Neis de Bucaramanga, Rio de Oro sector, Cesar.

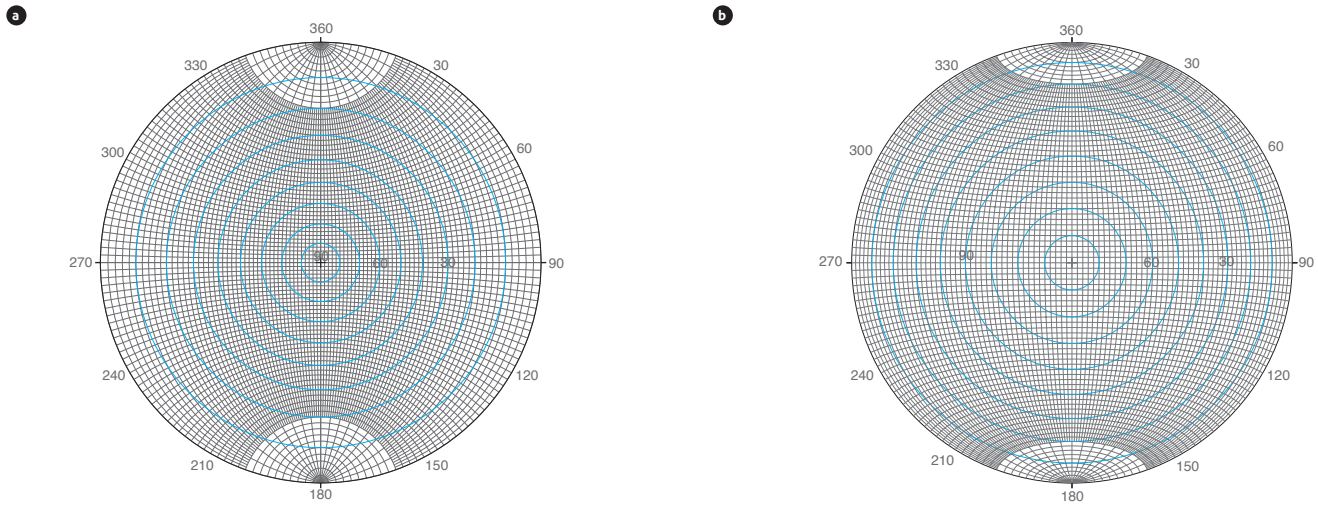

Figure 3. a) Modified Wulff stereographic projection grid, including concentric guiding circles (blue) for dip measurement and great circle plotting. b) Modified Schmidt equal-area projection grid, including concentric guiding circles (blue) for dip measurement and major circle plotting. c) Modified Schmidt equal-area projection grid, including concentric guiding circles (blue) for dip measurement and major circle plotting.

minor circles, which correspond to vertical planes that, in general, do not pass through the center of the sphere containing the equatorial plane, and form circles with increasing radius; the maximum radius constitutes the center of the sphere, or east-west line (Phillips, 1973). The intersection between the arcs representing the major circles and the arcs representing the minor circles gives rise to what is known as the *stereographic network* (Phillips, 1973). Starting from the construction of the stereographic net, minor circles parallel to the equatorial plane, projected from the nadir and similar to a polar stereographic net, can be included on the equatorial plane (Phillips, 1973). These circles are at a tangent to the major and minor circles defining the stereographic grid (Figure 3), and indicate a given inclination, which in the case of the modified stereographic grid represent divisions between 0° and 90°. Thus, any major circle arc of random bearing with defined inclination can be plotted tangentially to the equivalent concentric minor circle (Figure 4).

The procedure followed for graphically visualizing the spatial orientation of structural data acquired in the field depends on the convention or structural notation used for recording data during fieldwork (McClay, 1987). Relevant instructions for the stereographic projection of structural data are taken into account (Phillips, 1973; Marshak and Mitra, 1988; Lisle and Leyshon, 2004), which, in general terms, places the direction of the dip azimuth on the outer circle, and the dip or inclination on the inner circles, increasing the inclination from the edge towards the center. This facilitates the graphical representation of structural data acquired under the convention or notation of quadrants, strike azimuth, right hand rule, and dip azimuth or dip direction.

3.1 Procedures for graphical representation of data

1. The orientation is measured on the outer circle of the grid for modified stereographic projection. The circle can be divided into quadrants (northeast, northwest, southeast, and southwest), or it can be read in azimuth (0 to 360°). Each major division equals 10°.
2. The dip (inclination of the plane) is read on the inner circles, taking into account that it increases towards the center; that is, the lowest inclinations would be located on the outer edge, and the highest towards the center.
3. Quadrants. As an example, the notation N 58° E/70 °NW will be plotted. On the modified stereographic projection grid the location of the northwest (NW) quadrant is identified and the bearing is located by counting 58° from north to west on the outer circle. At 90° from the point where the bearing was found, in the northeast (NE) quadrant, the dip is measured on the inner circles towards the center, locating the circle equivalent to 70°. An arc (or cyclographic trace) is drawn which joins the notch of the bearing on the outer circle and the point corresponding to the dip on the appropriate inner circle (Figure 5a), to represent the spatial orientation of the plane.

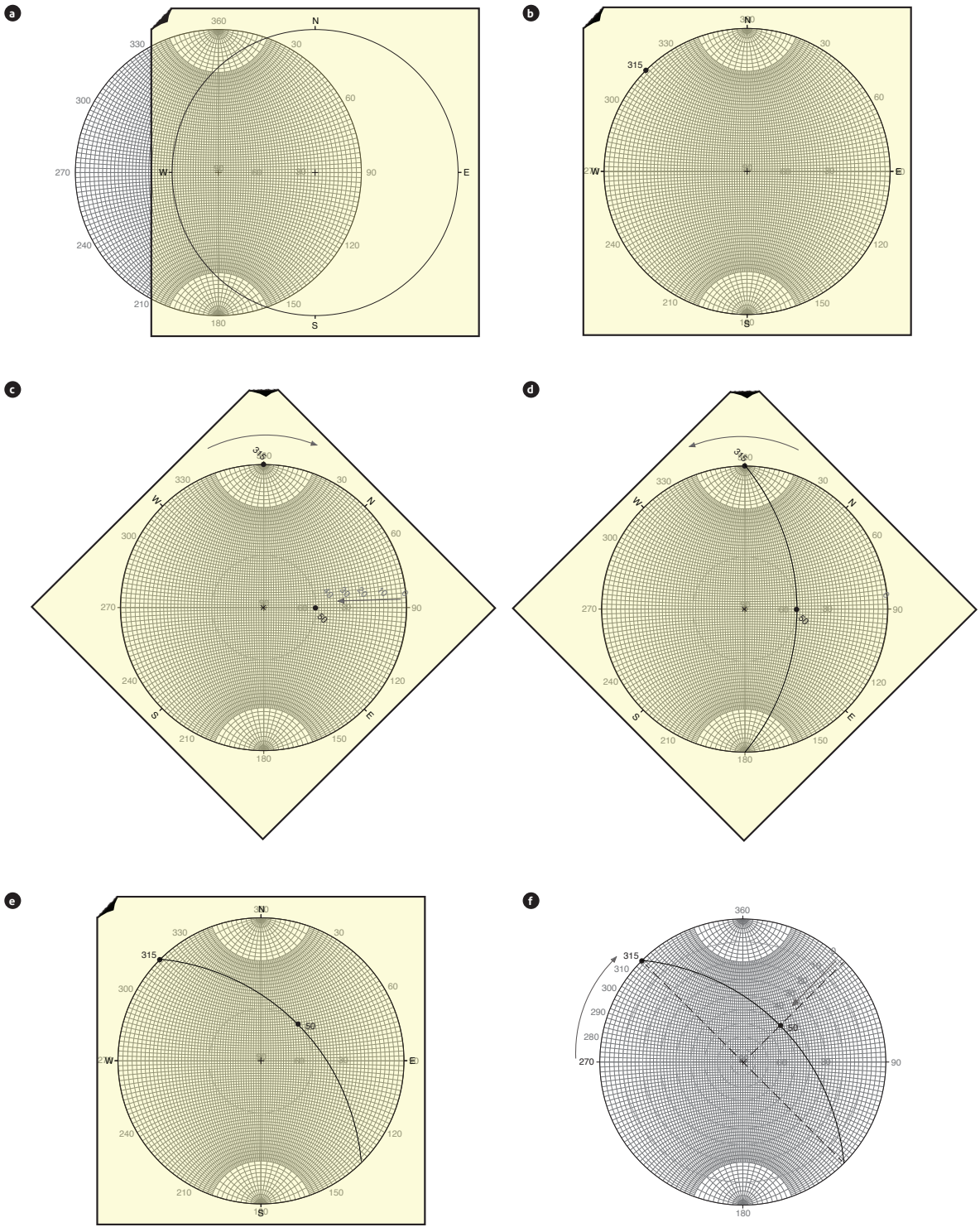

Figure 4. Traditional graphical representation of field-acquired structural data compared to the modified Wulff stereographic projection graph
a) Wulff stereographic projection grid and paper on which the structural datum 315/50 will be plotted. b) Location of the plane heading datum (315) in azimuth on the outer circle. c) Right turn of the paper until the plane heading (located on the outer circle) coincides with the north-south line of the projection grid or with the notch of 360°. d) Measurement of the dip or inclination of the plane from the outer circle inward to the notch indicating 50. e) Measurement of the dip or inclination of the plane from the outer circle inward to the notch indicating 50. f) Measurement of the plane heading (315) in azimuth on the outer circle to the notch indicating 50. Measurement of the dip or inclination of the plane from the outer circle to the inner circle, up to the notch indicating 50°. d) Trace the cyclograph along the major circle of the stereographic grid. e) Left turn of the paper to the starting point. f) Modified Wulff equal-area projection grid, in which the cyclographic trace and the pole of the cross-sectioned plane are shown directly; the cyclograph is tangent to the circle representing the 50° inclination.

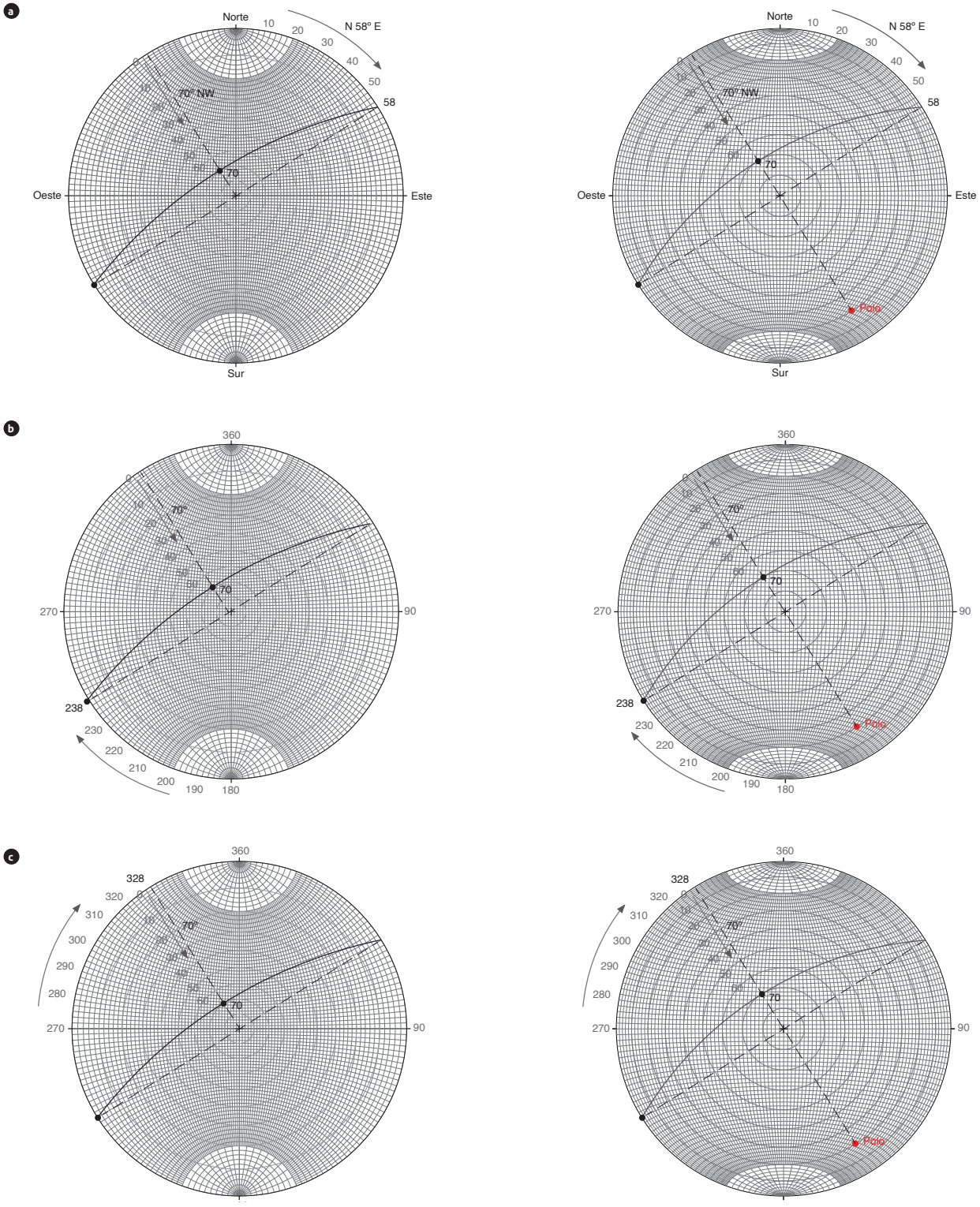

Figure 5. a) Graphical representation of structural data acquired in the field and recorded as quadrants on the modified stereographic projection grid. Left: modified Wulff stereographic projection grid. Right: modified Schmidt equal-area projection grid, showing the cyclographic trace and the plane pole. b) Graphical representation of structural data acquired in the field and recorded as heading azimuth over the modified stereographic projection grid. Left: modified Wulff stereographic projection grid. Right: modified Schmidt equal-area projection grid showing the cyclographic trace and plane pole. c) Graphical representation of structural data acquired in the field and recorded as Dip Direction (dip→dir) azimuth over the modified stereographic projection grid. Left: modified Wulff stereographic projection grid. Right: modified Schmidt equal-area projection grid, showing the cyclographic trace and the pole of the plane.

4. Azimuth of bearing (right hand ruler). As an example, the notation 238°/70° will be plotted. On the modified stereographic projection grid, the location of the bearing azimuth of 238° of a plane on the outer circle is identified. At 90 °and to the right of the point where the bearing was found, the dip is measured on the inner circles towards the center, locating the circle equivalent to 70°. An arc (or cyclographic trace) is drawn which joins the notch of the bearing on the outer circle and the point corresponding to the dip on the appropriate inner circle (Figure 5b), to represent the spatial orientation of the plane.
5. Dip direction azimuth. As an example, the notation 70°→328*° will be plotted. In the modified stereographic projection network, the location of the dip azimuth of 328° of a plane on the outer circle is identified. From this point the dip is measured on the inner circles towards the center, locating the circle equivalent to 70°. An arc (or cyclographic trace) is drawn which joins the point corresponding to the dip on the appropriate inner circle with the notch of the bearing on the outer circle (Figure 5c), to represent the spatial orientation of the plane. It should be noted that at 90°, counterclockwise and clockwise, and from the dip azimuth notch, notches can be located that would represent the strike of the plane on the outer circle.

4. Statistical determination of main structural data trends and their graphical representation

A rose plot, also known as a polar histogram, is a circular histogram of frequencies (Mardia, 1972; Davis, 2002; Borradaile, 2003; McKillup and Dyar, 2010; Singhal and Gupta, 2010; Davis et al. 2012; Sanderson and Peacock, 2020). It allows for a quick angular graphical display of the data (Marshak and Mitra, 1988; Kutty and Parthasarathi, 1992; Robson, 1994; Twiss and Moores, 2007) in areas where clarity is needed vis-à-vis the predominant principal structural trend of the fabric element of interest. This diagram is constituted by a radial distribution of lines dividing intervals of ranges of 10°, and concentric circles representing a percentage of data included in the ranges, which from the inside increase every 10 % up to the outer circle, which corresponds to 100 % (Figure 6). In such diagrams, the data are grouped into frequency intervals, converted to percentages and plotted as shaded wedge-shaped zones, called *petals*, in which the radius corresponds to the percentage value, and their orientation represents the predominant trend of orientation of the geological structures, which are directly related to the amount of data.

Preferential trends of planes and lines, such as families of joints, and structural trends of planes of different types, such as

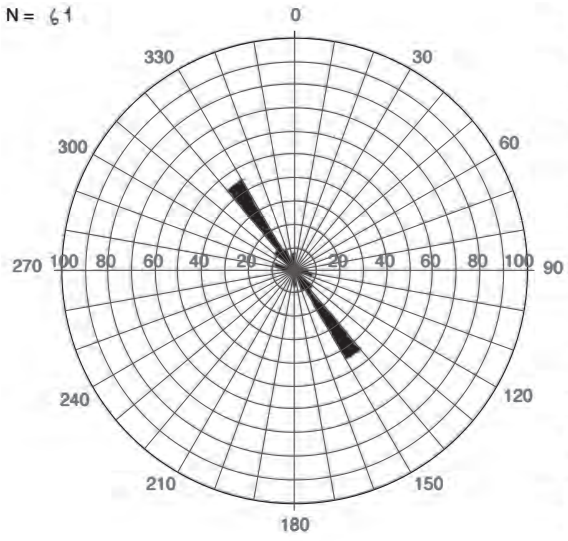

Data table for graphical representation in the strike

Total number of data (N): 61

Az. Range of Dip		Az. Range of Strike		Quadrants	Data	%
0-9	180-189	90-99	270-279	N 81-90 W	=3	5%
10-19	190-199	100-109	280-289	N 71-80 W	=5	8%
20-29	200-209	110-119	290-299	N 61-70 W		
30-39	210-219	120-129	300-309	N 51-60 W		
40-49	220-229	130-139	310-319	N 41-50 W	=7	11%
50-59	230-239	140-149	320-329	N 31-40 W	=27	44%
60-69	240-249	150-159	330-339	N 21-30 W	=10	10%
70-79	250-259	160-169	340-349	N 11-20 W		
80-89	260-269	170-179	350-359	N 01-10 W	=4	7%
90-99	270-279	0-9	180-189	N 00-09 E		
100-109	280-289	10-19	190-199	N 10-19 E		
110-119	290-299	20-29	200-209	N 20-29 E		
120-129	300-309	30-39	210-219	N 30-39 E		
130-139	310-319	40-49	220-229	N 40-49 E		
140-149	320-329	50-59	230-239	N 50-59 E		
150-159	330-339	60-69	240-249	N 60-69 E	=1	1%
160-169	340-349	70-79	250-259	N 70-79 E	=1	2%
170-179	350-359	80-89	260-269	N 80-89 E	=3	5%

Figure 6. Template for the graphical representation of structural data in a rose diagram, and an example of a table for the determination of the amount of data per class or interval, for its schematization by percentage
The structural data are grouped based on 10° intervals, corresponding to dip azimuth (Az. Dip Range), heading azimuth (Az. Heading Range), each with two columns of data between 0 °and 179°, and 180° and 359°, respectively, and quadrant. The data are grouped by classes in the "Data" column. In the final column, the percentage (%) is calculated by dividing the amount of data in the class by the total amount of data and then multiplying the result by 100.

S_0, S_1 to S_n, and S_{n+1} to S_{n+n}, as well as dikes, veins, and so on can be plotted on a rose diagram, and can also be used for the graphical representation of the preferential orientation of lineaments in remote sensing images. The rose diagram should be plotted by structural data type (S_0, S_1, S_n, or S_{n+n}) and include the amount of structural data represented in the plot. Traditionally, the construction of rose diagrams is performed using specialized software and mobile device applications for structural geology, such as Stereonet (Allmendinger, https://www.rickallmendinger.net). During fieldwork, it is crucial to visualize the main trends in strike and/or dip of the geological structure data so as to have control of the regional spatial distribution of the analyzed structures among the different rock bodies. Hence why it is important to construct this type of graph directly in the outcrop, as a complement to the construction of graphs by means of the modified stereographic projection network. For this purpose, a methodology is presented that facilitates the realization of this type of graph in the field, from structural data that are recorded by any of the structural notations.

According to the foregoing, the fieldwork prior to the elaboration of rose diagrams begins by grouping the structural data in classes measured in the outcrop, where the classes, for practical purposes, correspond to 10° intervals. Thus, the data are organized by classes in a table in which all possible data ranges included in the rose plot are included. The data ranges are included in three groups, which correspond to the structural notations of data measurement, and which in the table are equivalent to the dip azimuth (Az. Dip Range) and heading azimuth (Az. Heading Range) ranges, each with two columns with data between 0° and 179°, and between 180° and 359°, respectively, along with quadrants in which the data are organized in a single column (Figure 6). This grouping is arranged in such a way as to allow direct visualization of the equivalence between the types of structural notations, while favoring the grouping of axial data in 180° modes (Sanderson and Peacock, 2020). Once the data are grouped by classes in the "Data" column, the percentage (%) value is calculated by dividing the amount of data in the class by the total amount of data and multiplying the result by 100.

To construct the graph, the corresponding ranges are plotted and shaded in the rose diagram, with their respective percentages. For this, from the columns in the table that make up the heading azimuth range (Az. Heading Range), each of the classes with a percentage value is selected and associated with its respective 10° interval from the outer circle of the graph. Once this is done, the percentage value is plotted from the center to the edge within each interval, thus forming the wedges that correspond to the petals (Figure 6). One way to validate the diagram is to sum the plotted percentages, which should correspond to a total of 100. The rose diagram results in the graphical representation of the orientation, in which the petal with the highest percentage corresponds to the range that includes the preferential direction of the data, and shows trends with random distributions or with uniform directions. This diagram allows regional comparisons of the preferential orientation of different data set distributions (Sanderson and Peacock, 2020).

5. Discussion

The description and interpretation of all the fabric elements or structures present, at all scales, is one of the main inputs for the reconstruction of the geological and tectonic history of an area. In this sense, the mapping of structures directly in the field is conducive to the correct discrimination of the different fabric elements, either planar or linear, in addition to their measurement (either by using analog compasses or mobile devices) and visualization. When regional surveys are undertaken using analog compasses or mobile devices, the visualization of the data directly in the outcrop is fundamental for differentiating structural domains, validating tectonic drag directions, paleocurrent directions and structural trends, among others (Potter and Pettijohn, 1963; Nemec, 1988; Hatcher, 1995; Gabrielsen and Braathen, 2014; Abdunaser, 2015; Ahmadirouhani et al., 2017; Han et al., 2018; Rajasekhar et al., 2018). Considering that it is vital to know the arrangement of geological structures in an area by outcrop or station, the methodological implementation of the modified stereographic network approach presented herein constitutes a practical and innovative solution for the graphical representation of structural data when mapping in areas with broken, canyoned, or difficult to access topography, where there is no signal for the use of mobile devices to generate stereograms directly using apps. Also, the use of the proposed modified stereographic network allows the inclusion of stereograms and rose diagrams directly in the field notebook (e.g., if printed on sheets of adhesive paper) and simplifies the use of tracing paper, tables, stereographic projection diagrams and thumbtacks, which tend to be cumbersome and even impractical particularly when inclement weather prevails.

The use of analog compasses involves carefully obtaining readings and approximating each reading to the nearest degree

(Ragan, 2009). The accuracy of the readings depends on the location of the compasses in the correct position to perform the measurement on a surface, and on systematic errors, which can be induced by the use of erroneous angles for the correction of the data with respect to the magnetic declination, the presence of magnetic materials near or on the reading surface, or due to the presence of induced electromagnetic fields (Ragan, 2009). From the orderly and methodical recording of data it is possible to construct stereograms to verify the accuracy of the measurements made, mainly when developing data surveys of lineations related to planes, as is the case with structural data of slickenlines in faults or brittle shear zones, although there is software that allows minimizing the error by approximation to the nearest degree in office data processing, as is the case of Tectonics. The use of mobile devices with different operating systems (iOS or Android) for structural data acquisition facilitates the recording and visualization of orientation measurements of geological structures (Allmendinger et al., 2017; Novakova and Pavlis, 2017; Lee et al., 2018; Whitmeyer et al., 2019), and additionally allows many measurements to be taken quickly (Allmendinger, 2017; 2019). In some cases, these devices offer additional advantages in terms of accuracy in gauging the structural data and identifying the locations of field stations where the structural data measurements are taken using the positioning systems included in mobile devices which can be visualized on digital mapping platforms (e.g., Google Earth). Whether using analog compasses or mobile devices, a recording scheme is proposed that facilitates the direct association between plans and lineaments contained in them, from the incorporation of the data in a table, in which the planar surfaces and lineations will be distributed in adjacent columns, including the data and type of structure. This allows standardizing the data recording in an orderly and methodical way (see Table 1), especially when annotations of the measurements are made in notebooks.

Where measurements are taken using mobile devices or analog compasses, the graphical representation of the spatial orientation of structures is made on stereographic (Wulff) or equal-area (Schmidt) grids, using the projection on the lower hemisphere, which means that the observations are projected to the horizontal plane passing through the center of the sphere (Allmendinger, 2019). Visualization on stereograms is not only a good, but a necessary, practice when performing work involving the comparison of spatial orientations of structures between stations for the definition of structural domains or the direction of tectonic drag, among other factors. As already mentioned, the use of mobile devices has facilitated the graphic visualization of structural data. However, it is not always possible to use these devices in the field, which forces individuals to resort to manual construction of conventional graphic representations on tracing or transparent paper, although this is imprecise, and in many cases cumbersome and frustrating. The use of the stereographic or equal-area projection for the graphic representation of the spatial orientation of structures is determined by the data set; that is, if the densities of the plotted directions are important for the determination and analysis of preferred orientations, the equal-area projection should be used, since such a projection does not show the effect of area distortion (Lisle and Leyshon, 2004). However, the use of one or the other for the realization of geometric constructions is irrelevant, although the Wulff grid is more useful for graphical representations involving the cyclographic trace, and is used to determine the geometric relationships of structures (Phillips, 1973; Babín and Gómez, 2010d). Another form of two-dimensional visualization that complements the applications of stereograms for structural analysis is the representation of strike trends in structural data via rose diagrams, which, in the case of joints, for example, is important because of its relation to the orientation of the stress field.

The use of a modified network for the direct graphical representation of structural data in an outcrop, which allows dispensing with tracing or transparent paper, is a simple, efficient, and effective alternative solution to visualize the geometric relationships of fabric elements (planar and linear) during structural surveys involving comparisons of the spatial orientations of structures between stations or outcrops, in areas where it is not possible to use mobile devices for this purpose. The procedure proposed here to perform the graphical representation in the field is useful and innovative, can be applied with any type of structural notation, and serves as a complement to field studies in which it is necessary to differentiate structural domains, the direction of tectonic drag, the presence of local and regional folds, or the preliminary structural analysis, in which the stress field relationship is identified, among other aspects. For the visualization of data to determine the geometrical relationship between fabric elements, the Wulff stereographic network has been modified, while for the visualization of data involving the determination of preferential directions and their relationship to the stress field, the Schmidt network has been modified. Both graphical representations can be used to perform geometrical constructions and can be complemented with the representation of orientations in rose diagrams.

6. Conclusions

This article proposes a scheme for recording data acquired in the field in a table, which allows sorting by type of fabric element (planar or linear), and the recording of the lineations always in front of the plane that contains them. In addition, the recording scheme includes the data corresponding to the kinematics or direction of movement of faults and shear zones, the indicators that support the kinematics, and a qualitative assessment of the certainty or reliability of the kinematics assigned to the direction of movement of shear zones; this is essential for determining paleostress tensors through the application of software. This logging scheme constitutes a standard that can be implemented by students, researchers, and other professionals in geosciences, and has applications in structural analysis that, depending on the purpose, can be complemented with data specific to the objective, whether cartographic, geomechanical, geotechnical, or mining, among others.

The direct graphical representation of geological structure data in the field is realized by a fast method to visualize the data on modified Wulff and Schmidt grids, which allow the structural data to be plotted in the outcrop, dispensing with the use of tracing or transparent paper, regardless of the structural notation used. The visualization of the spatial orientation of planar and linear structures in modified stereographic projection diagrams is complemented with rose diagrams, to reveal and understand the probable relationships between the structures, and to facilitate understanding of the different phases of deformation recorded by the lithological units analyzed.

The use of the methodology proposed herein during field campaigns, can minimize human errors at the time of recording and manipulating data in the outcrops. The correct, methodical, and orderly implementation of data recording of the measurements made concerning the fabric elements (planar and linear) in the proposed table, whether obtained by using mobile devices or analog geological compasses, is fundamental for the analysis of the spatial distribution of the data directly in the outcrops. Further, implementation of the modified network for direct graphical representation and visualization of data in the field is innovative, and simplifies the use of tracing paper, making this process more effective and efficient. The use of stereographic or equal-area projection diagrams allows determining key structural trends and differentiating between structural domains, as well as determining the direction of tectonic drag, kinematics of faults and shear zones, and paleostress tensors, among other considerations, to support the reconstruction of the geologic and tectonic history of an area and the establishment of the relationships between different geologic processes.

Acknowledgments

This work was completed within the framework of the Tectonic Group, Dirección de Geociencias Básicas, Servicio Geológico Colombiano. The authors are grateful to the anonymous reviewers whose comments and suggestions helped to improve the manuscript. We also extend our gratitude to Sergio Adrián López Isaza and Luis Fernando Páez Sinuco for fruitful discussions concerning the practical implications of this technique.

References

Abdunaser, K. M. (2015). Satellite imagery for structural geological interpretation in Western Sirt Basin, Libya: Implication for petroleum exploration. *Geosciences*, *5*(1), 8-25.

Allmendinger, R. W. (2017). *Stereonet mobile for iOS v 3.0.* http://www.geo.cornell.edu/geology/faculty/RWA/programs/stereonet-mobile.html

Allmendinger, R. W. (2019). *Modern structural practice: A structural geology laboratory manual for the 21st Century.* http://www.geo.cornell.edu/geology/faculty/RWA/structure-lab-manual/

Allmendinger, R. W., Cardozo, N., & Fisher, D. (2012). *Structural geology algorithms: Vectors and tensors*. Cambridge University Press.

Allmendinger, R. W., Siron, C. R., & Scott, C. P. (2017). Structural data collection with mobile devices: Accuracy, redundancy, and best practices. *Journal of Structural Geology*, *102*, 98-112. https://doi.org/10.1016/j.jsg.2017.07.011

Ahmadirouhani, R., Rahimi, B., Karimpour, M. H., Malekzadeh S., A., Afshar N., S., & Pour, A. B. (2017). Fracture mapping of lineaments and recognizing their tectonic significance using SPOT-5 satellite data: A case study from the Bajestan area, Lut Block, east of Iran. *Journal of African Earth Sciences*, *134*, 600-612. https://doi.org/10.1016/j.jafrearsci.2017.07.027

Babín V., R. S., & Gómez O., D. (2010a). Problemas de geología estructural. 1. Conceptos generales. *Reduca (Geología), Serie Geología Estructural*, *2*(1), 1-10.

Babín V., R. S., & Gómez O., D. (2010b). Problemas de geología estructural. 2. Orientación y proyección de planos en el espacio. *Reduca (Geología), Serie Geología Estructural*, *2*(1), 11-23.

Babín V., R. S., & Gómez O., D. (2010c). Problemas de geología estructural. 3. Orientación y proyección de líneas en el espacio. *Reduca (Geología), Serie Geología Estructural*, *2*(1), 24-40.

Babín V., R. S., & Gómez O., D. (2010d). Problemas de geología estructural. 9. Análisis estructural mediante diagramas de contornos. *Reduca (Geología), Serie Geología Estructural*, *2*(1), 148-192.

Bartlett, W. L., Friedman, M., & Logan, J. M. (1981). Experimental folding and faulting of rocks under confining pressure. Part IX: Wrench faults in limestone layers. *Tectonophysics*, *79*(3-4), 255-277.

Blés, J. L. (1977). *La fracturation des roches. 2eme partie: Observation et interprétation des fractures naturelles*. Bureau de Recherches Géologiques et Minières, Service Géologique National, France.

Borradaile, G. (2003). *Statistics of earth science data*. Springer.

Bucher, W. H. (1944). Studies for students: The stereographic projection, a handy tool for the practical geologist. *The Journal of Geology*, *52*(3), 191-212. https://doi.org/10.1086/625206

Cardozo, N., & Allmendinger, R. W. (2013). Spherical projections with OSXStereonet. *Computers & Geosciences*, *51*, 193-205. https://doi.org/10.1016/j.cageo.2012.07.021

Chica S., A. (1984). *Análisis de estructuras geológicas*. Universidad Nacional de Colombia

Compton, R. R. (2016). *Geology in the field*. Earthspun Books.

Davis, J. C. (2002). *Statistics and data analysis in geology*. John Wiley & Sons Inc.

Davis, G. H., Reynolds, S. J., & Kluth, C. F. (2012). *Structural geology of rocks and regions*. John Wiley & Sons, Inc.

Delvaux, D., & Sperner, B. (2003). New aspects of tectonic stress inversion with reference to the Tensor program. In D. A. Nieuwland (ed.), *New insights into structural interpretation and modelling*. Special Publications, vol. 212. Geological Society of London. https://doi.org/10.1144/GSL.SP.2003.212

Doblas, M. (1987). Criterios del sentido de movimiento en espejos de fricción: Clasificación y aplicación a los granitos cizallados de la sierra de San Vicente (sierra de Gredos). *Estudios Geológicos*, *43*(1-2), 47-55.

Doblas, M. (1998). Slickenside kinematic indicators. *Tectonophysics*, *295*(1-2), 187-197. https://doi.org/10.1016/S0040-1951(98)00120-6

Doblas, M., Mahecha, V., Hoyos, M., & López Ruiz, J. (1997a). Slickenside and fault Surface kinematic indicators on active normal faults of the Alpine Betic cordilleras, Granada, southern Spain. *Journal of Structural Geology*, *19*(2), 159-170. https://doi.org/10.1016/S0191-8141(96)00086-7

Doblas, M., Faulkner, D., Mahecha, V., Aparicio, A., López Ruiz, J., & Hoyos, M. (1997b). Morphologically ductile criteria for the sense of movement on slickensides from an extensional detachment fault in southern Spain. *Journal of Structural Geology*, *19*(8), 1045-1054. https://doi.org/10.1016/S0191-8141(97)00032-1

Fossen, H. (2010). *Structural geology*. Cambridge University Press.

Fossen, H. (2019). Writing papers with an emphasis on structural geology and tectonics: advices and warnings. *Brazilian Journal of Geology*, *49*(4). https://doi.org/10.1590/2317-4889201920190109

Fossen, H., Cavalcante, G. C. G., Pinheiro, R. V. L., & Archanjo, C. J. (2019). Deformation: progressive or multiphase? *Journal of Structural Geology*, *125*, 82-99. https://doi.org/10.1016/j.jsg.2018.05.006

Gabrielsen, R. H., & Braathen, A. (2014). Models of fracture lineaments: joint swarms, fracture corridors and faults in crystalline rocks, and their genetic relationships. *Tectonophysics*, *628*, 26-44. https://doi.org/10.1016/j.tecto.2014.04.022

Ghosh, S. K. (2013). *Structural geology: fundamentals and modern developments*. Pergamon Press.

Han, L., Liu, Z., Ning, Y., & Zhao, Z. (2018). Extraction and analysis of geological lineaments combining a DEM and remote sensing images from the northern Baoji loess area. *Advances in Space Research*, *62*(9), 2480-2493. https://doi.org/10.1016/j.asr.2018.07.030

Hancock, P. L. (1985). Brittle microtectonics: Principles and practice. *Journal of Structural Geology*, *7*(3-4), 437-457. https://doi.org/10.1016/0191-8141(85)90048-3

Hanmer, S., & Passchier, C. (1991). *Shear-sense indicators: A review*. Geological Survey of Canada, Paper 90-17.

Hatcher, R. D. Jr. (1995). *Structural geology: Principle, concepts and problems*. Prentice Hall.

Hills, E. S. (1972). *Elements of structural geology* (2nd ed.). Chapman and Hall, Ltd.

Holcombe, R. J. (2015). GEOrient v.9.5.1. Department of Earth Sciences, University of Queensland, Australia. http://www.holcombe.net.au/software/

Hopgood, A. M. (1999). *Determination of structural successions in migmatites and gneisses*. Springer Science + Busines Media, B. V. https://doi.org/10.1007/978-94-011-4427-8

Hobbs, B. E., Means, W. D., & William, P. E. (1976). *An outline of structural geology*. John Wiley & Sons, Inc.

Kutty, T. S., & Parthasarathi, G. (1992). Rose.C- A program in "C" for producing high-quality rose diagrams. *Computers & Geosciences, 18*(9), 1195-1211. https://doi.org/10.1016/0098-3004(92)90040-X

Lisle, R. J., & Leyshon, P. R. (2004). *Stereographic projection techniques for geologist and civil engineers*. Cambridge University Press. https://doi.org/10.1017/CBO9781139171366

Lee, S., Suh, J., & Choi, Y. (2018). Review of smartphone applications for geoscience: Current status, limitations, and future perspectives. *Earth Science Informatics*, 11, 463-486. https://doi.org/10.1007/s12145-018-0343-9

López I., J. A., & Zuluaga C., C. A. (2012). Neis de Macuira: Evolución tectónica de las rocas metamórficas paleozoicas de la alta Guajira, Colombia. *Boletín de Geología*, *34*(2), 15-36.

Mardia, K. V. (1972). *Statistics of directional data*. Academic Press, Inc.

Marrett, R. A., & Allmendinger, R. W. (1990). Kinematic analysis of fault-slip data. *Journal of Structural Geology*, *12*(8), 973-986. https://doi.org/10.1016/0191-8141(90)90093-E

Marshak, S., & Mitra, G. (1988). *Basic methods of structural geology*. Prentice Hall.

Mawer, C. K. (1992). Kinematic indicators in shear zones. In M. J. Bartholomew, D. W. Hyndman, D. W. Mogk, and R. Mason (eds.), *Basement tectonics 8: Characterization and comparison of ancient and Mesozoic continental margins: Proceedings of the 8th International Conference on Basement Tectonics (Butte, Montana, 1988)*. Kluwer Academic Publishers. https://doi.org/10.1007/978-94-011-1614-5

McClay, K. R. (1987). *The mapping of geological structures*. John Wiley & Sons.

McKillup, S., & Dyar, M. D. (2010). *Geostatistics explained: An introductory guide for earth scienctists*. Cambridge University Press. https://doi.org/10.1017/CBO9780511807558

Nemec, W. (1988). The shape of the rose. *Sedimentary Geology*, *59*(1-2), 149-152.

Novakova, L., & Pavlis, T. L. (2017). Assessment of the accuracy of smart phones and tablets for measurement of planar orientations: A case study. *Journal of Structural Geology*, 97, 93-103. https://doi.org/10.1016/j.jsg.2017.02.015

Ortner, H., Reiter, F., & Acs, P. (2002). Easy handling of tectonic data: The programs TectonicVB for Mac and TectonicsFP for Windows™. *Computers & Geosciences, 28(10)*, 1193-1200. https://doi.org/10.1016/s0098-3004(02)00038-9

Passchier, C. W., & Trouw, R. A. J. (2005). *Microtectonics*. Springer Science and Business Media. https://doi.org/10.1007/3-540-29359-0

Passchier, C. W., & Coelho, S. (2006). An outline of shear-sense analysis in high-grade. *Gondwana Research*, *10*(1-2), 66-76. https://doi.org/10.1016/j.gr.2005.11.016

Passchier, C. W., Myers, J. S., & Kröner, A. (1990). *Field geology of high-grade gneiss terrains*. Springer-Verlag. https://doi.org/10.1007/978-3-642-76013-6

Petit, J. P. (1987). Criteria for the sense of movement on fault surfaces in brittle rocks. *Journal of Structural Geology*, *9*(5-6), 597-608. https://doi.org/10.1016/0191-8141(87)90145-3

Petit, J. P., Proust, F., & Tapponnier, P. (1983). Critèriesde sens de movement sur les miroirs de failles en roches non calcaires. *Bulletin de la Société Ggéologique de France*, *XXV*(4), 589-608. https://doi.org/10.2113/gssgfbull.S7-XXV.4.589

Phillips, F. C. (1973). *La aplicación de la proyección estereográfica en geología estructural.* Trans.: C. M. Escorza (1975). Blume.

Potter, P. E., & Pettijohn, F. J. (1963). *Statistics of directional data*. Academic Press.

Price, N. J., & Cosgrove, J. W. (1990). *Analysis of geological structures*. Cambridge University Press.

Ragan, D. M. (2009). *Structural geology: An introduction to geometrical techniques*. Cambridge University Press.

Rajasekhar, M., Sudarsana R., G., Siddi R., R., Ramachandra, M., & Pradeep K., B. (2018). Data on comparative studies of lineaments extraction from ASTER DEM, SRTM, and Cartosat for Jilledubanderu River basin, Anantapur district, A. P, India by using remote sensing and GIS. *Data in Brief*, 20, 1676-1682. https://doi.org/10.1016/j.dib.2018.09.023

Ramsay, J. G. (1967). *Folding and fracturing of rocks*. McGraw-Hill Book Company.

Roberts, J. L. (1982). *Introduction to geological maps and structures*. Pergamon Press.

Robson, R. M. (1994). A multi-component rose diagram. *Journal of Structural Geology*, *16*(7), 1039-1040. https://doi.org/10.1016/0191-8141(94)90086-8

Sander, B. X. (1911). Über Zusammenhänge zwischen Teilbewegung und Gefüge in Gesteinen. *Tschermaks Mineralogische und Petrographische Mitteilungen*, 30, 281-314. https://doi.org/10.1007/BF02994467

Sander, B. (1970). *An introduction to the study of fabrics of geological bodies*. Pergamon Press.

Sanderson, D. J., & Peacock, D. C. P. (2020). Making rose diagrams fit-for-purpose. *Earth-Science Reviews*, 201, 103055. https://doi.org/10.1016/j.earscirev.2019.103055

Simpson, C., & Schmid, S. M. (1983). An evaluation of criteria to deduce the sense of movement in sheared rocks. *GSA Bulletin*, *94*(11), 1281-1288. https://doi.org/10.1130/0016-7606(1983)94<1281:AEOCTD>2.0.CO;2

Singhal, B. B. S., & Gupta, R. P. (2010). *Applied hydrogeology of fractured rocks*. Springer. https://doi.org/10.1007/978-90-481-8799-7

Sugden, T. (1987). Kinematic indicators: Structures that record the sense of movement in mountain chains. *Geology Today*, *3*(3-4), 93-99. https://doi.org/10.1111/j.1365-2451.1987.tb00496.x

Turner, F. J., & Weiss, L. E. (1963). *Structural analysis of metamorphic tectonites*. McGraw-Hill Book Company, Inc.

Twiss, R. J., & Moores, E. M. (2007). *Structural geology*. W. H. Freeman and Company.

Wilson, G. (1982). *Introduction to small-scale geological structures*. George Allen & Unwin. https://doi.org/10.1007/978-94-011-6838-0

Whitmeyer, S. J., Pyle, E. J., Pavlis, T. L., Swanger, W., & Roberts, L. (2019). Modern approaches to field data collection and mapping: Digital methods, crowdsourcing, and the future of statistical analyses. *Journal of Structural Geology*, *125*, 29-40. https://doi.org/10.1016/j.jsg.2018.06.023

Van der Pluijm, B. A., & Marshak, S. (2004). *Earth Structure: An introduction to structural geology and tectonics*. W. W. Norton & Company.

Žalohar, J. (2020). *T-Tecto Studio X5. Integrated software for structural analysis of earthquake focal-machanism and fault-slip data*. Introductory tutorial. Quantectum.

Žalohar, J., & Vrabec, M. (2007). Paleostress analysis of heterogeneous fault-slip data: The Gauss method. *Journal of Structural Geology, 29*(11), 1798-1810. https://doi.org/10.1016/j.jsg.2007.06.009